152. Crystal Structure and ESR Study of a Bimetallic Copper/Iron Crown Ether Inclusion Complex

by **Peter A. Chetcuti***, **André Liégard, Grety Rihs,** and **Günther Rist**

Central Research Laboratories, *Ciba-Geigy Ltd.*, CH-4002 Basel

and **Arthur Schweiger**

Laboratory for Physical Chemistry, Swiss Federal Institute of Technology, CH-8092 Zürich

(19.VII.91)

Bimetallic inclusion complexes have been synthesized by a secondary coordination interaction between the guest complex $[Fe(\eta^5\text{-}C_5H_5)(CO)_2(NH_3)][PF_6]$ and copper(II) complex **1a** or nickel(II) complex **1b** containing crown-ether hosts. The X-ray crystal-structure analysis established that the Cu, Fe inclusion complex **2** crystallizes as a centrosymmetric dimer with a Cu–Cu separation of 3.73 Å and a novel out-of-plane Cu–N interaction. The magnetic parameters for **2** were obtained by ESR and ENDOR spectroscopy. ESR susceptibility measurements down to 6 K exclude the presence of any antiferromagnetic coupling interaction between the Cu^{II} centers of the dimer.

Introduction. – Crown ethers are known to act as hosts to transition-metal complexes bearing ligands capable of H-bonding to the crown-ether O-atoms [1]. We were interested in making use of this interaction to synthesize bimetallic inclusion complexes using organometallic complexes as guest molecules and metal-containing crown ethers as hosts. The recently synthesized [2] crown-ether macrocycles **1** containing a transition-metal ion held by a *Schiff*-base moiety appeared to be suitable metal-containing hosts for this purpose. We wish to report the formation of such bimetallic inclusion complexes by interaction of the transition-metal ammine complex $[Fe(\eta^5\text{-}C_5H_5)(CO)_2(NH_3)][PF_6]$ with the crown-ether hosts **1a** and **1b**. The single-crystal X-ray structure determination of the complex $[\{Fe(\eta^5\text{-}C_5H_5)(CO)_2(NH_3)\} \subset \mathbf{1a}][PF_6]$ (**2**) revealed the expected Cu, Fe bimetallic inclusion complex which crystallized as a centrosymmetric dimer having a Cu–Cu

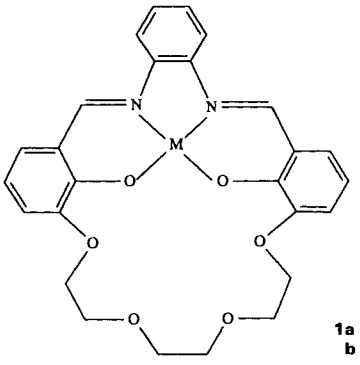

1a M = Cu
b M = Ni

distance of 3.73 Å. An electron spin resonance (ESR) and electron nuclear double resonance (ENDOR) study was carried out and the magnetic parameters of the complex obtained.

Results and Discussion. – *Molecular Structure of Inclusion Complex* **2**. The secondary coordination interaction between $[Fe(\eta^5\text{-}C_5H_5)(CO)_2(NH_3)][BPh_4]$ and dibenzo[18]crown-6 in solution has already been observed by IR and ^{1}H-NMR spectroscopy [1b]. Crystals of complex $[\{Fe(\eta^5\text{-}C_5H_5)(CO)_2(NH_3)\} \subset$ **1a**$][PF_6]$ (**2**) were obtained after allowing a solution of the two components to stand in the dark for ten days. A single-crystal X-ray diffraction study established the molecular structure of **2** to be the expected inclusion complex (*Figs. 1* and *2*). Selected bond lengths and bond angles for **2** are listed in *Table 1*. The guest complex is coordinated to the crown-ether host by a H-bonding interaction between the crown-ether O-atoms and the ammine H-atoms. The ammine ligand adopts a perching mode of coordination [4] in which the N(20) atom is positioned 1.22 Å above the best mean plane containing the six O-atoms which lie within 0.19 Å of this plane. The ammine group forms six bifurcated H-bonds with the crown-ether O-atoms, and the N(20)–O bond distances of the NH···O bonds fall in the range 2.89 to 3.13 Å, representing somewhat shorter H-bonds than usually observed for transition-metal ammine complexes with crown ethers [1a]. The coordination about the Cu-atom is distorted from planar, and adjacent phenyl rings subtend angles of 2 and 16° to one another. This distortion may be a consequence of the interaction between the phenolic O-atoms of the host and the ammine ligand of the guest complex, as observed in the interactions of these macrocycles with barium dication [2].

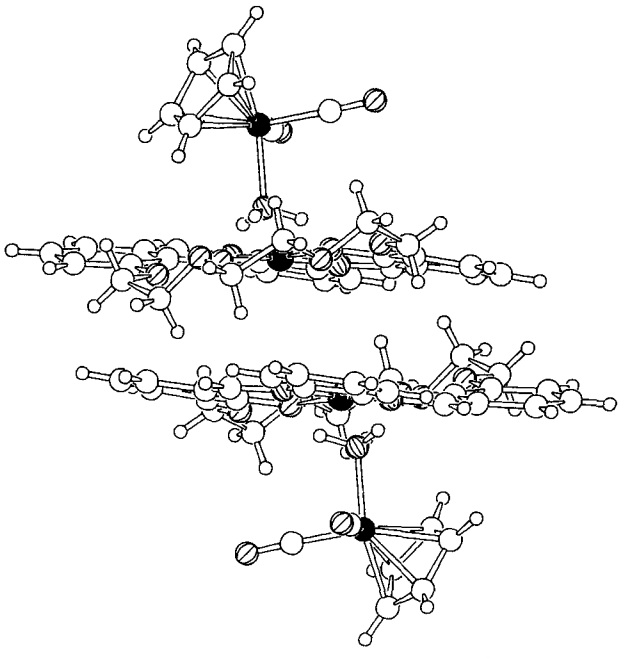

Fig. 1. *Molecular structure of the cationic bimetallic inclusion complex* $[\{Fe(\eta^5\text{-}C_5H_5)(CO)_2(NH_3)\} \subset$ **1a**$][PF_6]$ (**2**) *shown as a centrosymmetric dimer*. Hexafluorophosphate anions are omitted for clarity [3].

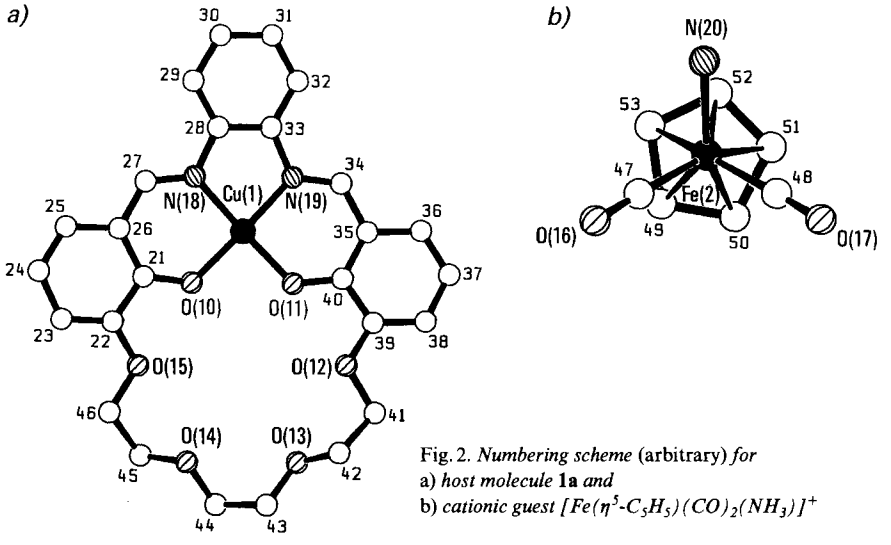

Fig. 2. *Numbering scheme* (arbitrary) *for*
a) *host molecule* **1a** *and*
b) *cationic guest* $[Fe(\eta^5\text{-}C_5H_5)(CO)_2(NH_3)]^+$

Table 1. *Bond Lengths* [Å] *and Bond Angels* [°] *for Inclusion Complex* **2**

Cu(1)–O(10)	1.899(5)	O(12)–C(41)	1.441(7)	C(28)–C(33)	1.415(9)
Cu(1)–O(11)	1.892(4)	O(13)–C(42)	1.42(1)	C(29)–C(30)	1.38(1)
Cu(1)–N(18)	1.935(5)	O(13)–C(43)	1.464(9)	C(30)–C(31)	1.41(1)
Cu(1)–N(19)	1.936(5)	O(14)–C(44)	1.426(9)	C(31)–C(32)	1.382(9)
Fe(2)–N(20)	2.008(6)	O(14)–C(45)	1.45(1)	C(32)–C(33)	1.395(9)
Fe(2)–C(47)	1.771(6)	O(15)–C(22)	1.361(7)	C(34)–C(35)	1.441(8)
Fe(2)–C(48)	1.789(7)	O(15)–C(46)	1.434(8)	C(35)–C(36)	1.43(1)
Fe(2)–C(49)	2.084(8)	O(16)–C(47)	1.143(8)	C(35)–C(40)	1.410(9)
Fe(2)–C(50)	2.09(1)	O(17)–C(48)	1.131(9)	C(36)–C(37)	1.37(1)
Fe(2)–C(51)	2.097(8)	N(18)–C(27)	1.300(9)	C(37)–C(38)	1.42(1)
Fe(2)–C(52)	2.120(7)	N(18)–C(28)	1.418(8)	C(38)–C(39)	1.39(1)
Fe(2)–C(53)	2.106(8)	N(19)–C(33)	1.416(7)	C(39)–C(40)	1.419(8)
P(3)–F(4)	1.577(5)	N(19)–C(34)	1.304(8)	C(41)–C(42)	1.52(1)
P(3)–F(5)	1.576(6)	C(21)–C(22)	1.436(9)	C(43)–C(44)	1.50(1)
P(3)–F(6)	1.586(5)	C(21)–C(26)	1.423(8)	C(45)–C(46)	1.50(1)
P(3)–F(7)	1.578(6)	C(22)–C(23)	1.39(1)	C(49)–C(50)	1.40(1)
P(3)–F(8)	1.554(6)	C(23)–C(24)	1.410(9)	C(49)–C(53)	1.46(1)
P(3)–F(9)	1.563(7)	C(24)–C(25)	1.37(1)	C(50)–C(51)	1.46(1)
O(10)–C(21)	1.304(8)	C(25)–C(26)	1.434(9)	C(51)–C(52)	1.42(1)
O(11)–C(40)	1.307(8)	C(26)–C(27)	1.417(9)	C(52)–C(53)	1.40(1)
O(12)–C(39)	1.366(8)	C(28)–C(29)	1.394(9)		
O(10)–Cu(1)–O(11)	88.9(2)	O(11)–Cu(1)–N(18)	172.1(2)	N(20)–Fe(2)–C(47)	93.5(3)
O(10)–Cu(1)–N(18)	93.6(2)	O(11)–Cu(1)–N(19)	93.8(2)	N(20)–Fe(2)–C(48)	94.9(3)
O(10)–Cu(1)–N(19)	172.3(2)	N(18)–Cu(1)–N(19)	84.7(2)	C(47)–Fe(2)–C(48)	92.8(3)
Cu_2N_2 moiety of a dimer					
Cu(1)–N(18)	1.935(5)	Cu(1)–N(18)–Cu(1′)	88.7(2)		
Cu(1)–N(18′)	3.239(6)	N(18)–Cu(1)–N(18′)	91.3(2)		
Cu(1)–Cu(1′)	3.734(1)				

An interesting feature of this structure is that it crystallizes as a centrosymmetric dimer in which the two Cu^{II} ions are 3.73 Å from each other; the structure in the solid state could be described as a Cu_2Fe_2 tetramer. The two best planes containing the aromatic *Schiff*-base moieties are 3.34 Å from each other, and dimer formation is probably enhanced by favorable π–π interactions. The tendency for planar *Schiff*-base metal complexes having a N_2O_2 set of donor ligands to form dimeric structures in solution [5] and in the solid state [6] *via* bridging O-atoms is well established. What is novel about the structure of **2** with respect to the structures of other planar *Schiff*-base metal complexes is that it is the imine N-atom of the *Schiff*-base moiety that appears to act as a weakly bridging atom, rather than the phenolic O-atom as observed in all other *Schiff*-base Cu^{II} dimers of this type [7]. The imine N-atom occupies an axial position with respect to the Cu-atom of the second macrocycle such that the N–Cu–N′ intermolecular bond angle is 88.7° and the out-of-plane Cu–N distance is 3.24 Å (see *Table 1*). This can at best only represent a weak interaction when compared to the axial Cu–O distance of 2.43 Å reported for bis(*N*-methylsalicylaldiminato)copper(II) ([Cu(Mesal)$_2$]) [6a] and 2.41 Å for [*N,N′*-ethylenebis(salicylideneiminato)]copper(II) ([Cu(salen]) [6d]. The Cu–Cu distance of 3.73 Å for complex **2** is considerably longer when compared to that of [Cu(Mesal)$_2$] [6a] (3.2 Å) and [Cu(salen)] (3.18 Å) [6d]. The unexpected Cu_2N_2 bridging system observed may be due to the reduction of electron density at the atoms O(10) and O(11) of the macrocycle as a result of the H-bonding interaction with the ammine ligand of the guest $[Fe(\eta^5\text{-}C_5H_5)(CO)_2(NH_3)]^+$ cation [1a]. The withdrawal of electron density from the crown-ether O-atoms to the guest iron complex is evidenced by a strong reduction of the carbonyl absorption frequencies of the guest in the solid state and in solution[1]). Furthermore, the molecular structures of the $CHCl_3$ adduct of [Cu(salen)] [8] reveal that the H-bonding interaction of a solvent molecule to a phenolic O-atom of the salen ligand not involved in dimer formation significantly lengthens the out-of-plane bond between the other phenolic O-atom of the [Cu(salen)] and the Cu-atom of the adjacent molecule of the dimer: the out-of-plane Cu–O bond distance of [Cu(salen)] increases from 2.41 to 2.79 Å as a result of this H-bonding. The hemihydrate of *N,N′*-ethylenebis(acetylacetoneiminato)copper(II) [9] and the 4-nitrophenol adduct of [Cu(salen)] [10] involve particularly strong H-bonds to the phenolic O-atom such that the Cu–O out-of-plane interaction is weakened to a point that dimer formation is no longer considered to occur. It appears that H-bonding between the ammine ligand of the guest iron complex and the atoms O(10) and O(11) of the macrocycle **1a** prevent the O-atoms from participating in a bridging interaction with the Cu^{II} ions and thus, the observed structure is in part a consequence of the inclusion of the guest iron complex.

ESR Studies with Magnetically Diluted Complex. In order to characterize the delocalization of the unpaired electron on the Cu-atom onto the aromatic ligand, complex **2** was magnetically diluted by substitution into the isomorphous lattice of the analogous nickel complex $[\{Fe(\eta^5\text{-}C_5H_5)(CO)_2(NH_3)\} \subset \mathbf{1b}][PF_6]$ (**3**) ([Cu]/[Ni] ≈ 1:100). The magnetic parameters obtained by ESR and pulsed ENDOR experiments for the diluted Cu^{II} complex are listed in *Table 2* together with data of related compounds. The ESR powder

[1]) The IR carbonyl absorption frequencies (KBr) of complex $[Fe(\eta^5\text{-}C_5H_5)(CO)_2(NH_3)][BPh_4]$ at 2060 and 2010 cm^{-1} shift to 2035 and 1985 cm^{-1} in the inclusion complex $[\{Fe(\eta^5\text{-}C_5H_5)(CO)_2(NH_3)\} \subset \mathbf{1a}][BPh_4]$. A similar decrease in the wavenumber is observed with the same complex in CH_2Cl_2 solution with dibenzo[18]crown-6 (see [1b]).

Table 2. *Magnetic Parameters for the Inclusion Complex [{Fe(η^5-C_5H_5)(CO)$_2$(NH_3)} ⊂ **1a**] (**2**)*

Coupling	Metal complex	∥[a])	⊥[b])	Isotropic
g (*Zeeman* coupling)	**2**	2.193[c])	2.051[d])	2.089[e])
	[Cu(salen)][h])	2.192	2.042	
A^{Cu} [MHz]	**2**	− 615[c])	− 103[d])	− 266[e])
	[Cu(salen)][h])	− 603	− 89	
A^{N} [MHz]	**2**	37.6[f])	*ca.* 43[g])	*ca.* 41
	[Cu(salen)][h])	38.9	37.1[i]), 50.5[i])	
	[Cu(salph)]	37.9[f])		
A^{H} [MHz]	**2**	17.5[f])	21.0[g])	*ca.* 19.8
	[Cu(salen)][h])	18.5	19.4[i]), 23.2[i])	
Q^{N} [MHz]	**2**	0.33[f])		
	[Cu(salen)][h])	0.44		

[a]) Coupling constants parallel to the principle axis of **2**.
[b]) Coupling constants perpendicular to the principle axis of **2**.
[c]) ESR powder spectrum of **2** diluted in an isomorphous lattice of the Ni^{II} complex [{Fe(η^5-C_5H_5)(CO)$_2$(NH_3)} ⊂ **1b**][PF_6] (**3**).
[d]) Estimated using the isotropic coupling constants.
[e]) ESR spectrum in toluene solution.
[f]) Pulsed ENDOR spectrum with single crystal type resolution. Contributions arising from mainly one orientation.
[g]) Data from pulsed ENDOR spectrum, average value in the plane of the complex.
[h]) Single-crystal data of [Cu(salen)] substituted in [Ni(salen)] [11].
[i]) Principle values in the plane of the metal complex.

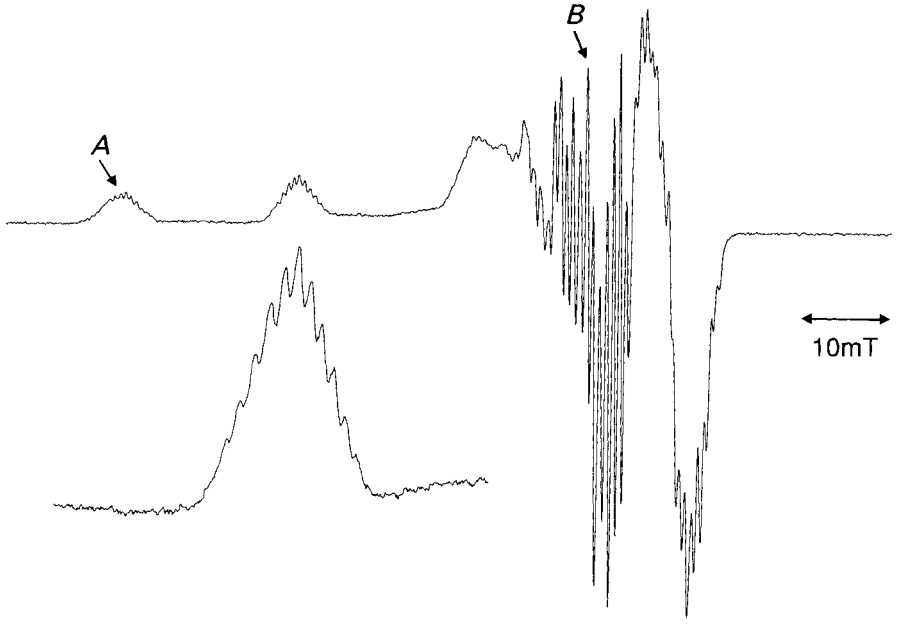

Fig. 3. *ESR powder spectrum of* **2** *diluted in an isomorphous lattice of the analogous nickel complex* **3**. ENDOR spectra were run at the two settings *A* and *B* indicated by the arrows. The absolute scale is given by $g_{\parallel} = 2.193$ and the low-field turning points.

spectrum of the diluted Cu^{II} complex (*Fig. 3*) is typical of an approximately planar Cu^{II} complex. The g-tensor and the Cu hyperfine tensor A^{Cu} are assumed to be axial and coaxial to one another. The parameters $g_\parallel$ and $A_\parallel^{Cu}$, corresponding to an orientation of the magnetic field parallel to the main molecular axis (perpendicular to the plane of the metal complex), were obtained from the ESR powder spectrum (*Fig. 3*); $g_\perp$ and $A_\perp^{Cu}$ (average in plane values) were estimated with the help of the isotropic coupling constants measured in toluene solution. The splittings of the $g_\parallel$ features in the low-field section of the ESR powder spectrum (*Fig. 3*) were assigned to the vinylic protons and the two N-atoms with an N hyperfine coupling approximately twice as large as that of the protons. This relationship leads to an eleven-line pattern with theoretical intensities 1:2:3:4:5:6:5:4:3:2:1. From the pronounced splitting observed in the high-field region ($g_\perp$ feature), the corresponding average values in the plane of the metal complex were obtained. The H hyperfine coupling $A^H(g_\parallel)$ and $A^H(g_\perp)$ are slightly smaller than those reported for the vinylic protons measured for complex [Cu(salen)] [12].

The N hyperfine and quadrupole coupling constants were obtained by a pulsed ENDOR experiment [13]. ENDOR transition frequencies along the principal hyperfine tensor axes of a single N-atom or of two equivalent N-atoms are given by the first-order equation (*Eqn. 1*).

$$\nu^N = \frac{1}{2} \cdot A^N \pm \nu_O^N \pm \frac{3}{2} \cdot Q^N \tag{1}$$

where ν_O^N is the frequency of the free N-nucleus[2]). The hyperfine coupling $A^N(g_\parallel)$, obtained from the single crystal type ENDOR spectrum [11] (*Fig. 4a*) by observing the low-field turning point of the ESR display (arrow *A* in *Fig. 3*), is close to the value of the same parameter for [Cu(salen)] [12] and almost equal to the value for *N,N'*-phenylenebis(salicylideneiminato)copper(II) ([Cu(salph)]) [14]. It has been shown that a value of $A^N(g_\parallel)$ between 36 and 39 MHz is characteristic for *cis*-N_2O_2 Cu-complexes with sp^2-type N-atoms [14]. The N hyperfine tensor of [Cu(salen)] is nearly axial with a small orthorhombic component [12a], this near-axial symmetry is reported for many other

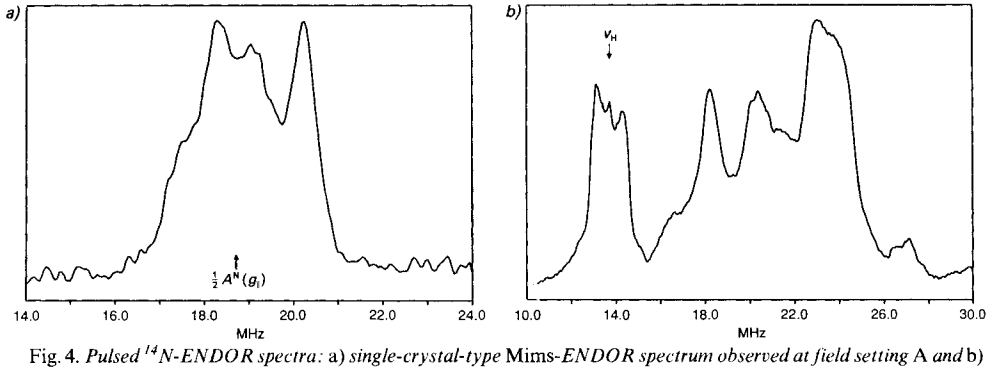

Fig. 4. *Pulsed ^{14}N-ENDOR spectra:* a) *single-crystal-type* Mims-*ENDOR spectrum observed at field setting* A *and* b) *powder* Davies-*ENDOR spectrum observed at field setting* B

[2]) For a strictly planar complex and a magnetic field oriented along the main axis of the molecule, the two N-nuclei should be equivalent. Incomplete resolution observed in the ENDOR spectrum is probably due to the slight tetrahedral distortion about the Cu-atom as observed in the molecular structure of the complex.

Cu-complexes with N-ligands [15]. The in-plane hyperfine coupling constant $A^N(g_\perp)$ was estimated from the ENDOR spectrum (*Fig. 4b*) measured in the $g_\perp$ region of the ESR powder spectrum as indicated by arrow *B* in *Fig. 3*. This measurement yielded a mean value for the in-plane hyperfine coupling constants which is in agreement with the value reported for [Cu(salen)] [12]. The nuclear quadrupole coupling constant $Q^N(g_\parallel)$ is again close to the value found for [Cu(salen)]. ENDOR transitions of the vinylic proton could not be observed, one of the transitions being buried by the N-spectrum and the other was too low in frequency to be measured by the spectrometer used. The good correspondence between the magnetic parameters obtained for the inclusion complex **2** and other similar *Schiff*-base systems, in particular [Cu(salph)], suggests that the crown-ether ring system and the secondary coordination of the iron complex $[Fe(\eta^5\text{-}C_5H_5)(CO)_2(NH_3)][PF_6]$ do not significantly perturb the spin delocalization on the aromatic system since this would be reflected in significant changes in the hyperfine coupling constants [14].

ESR Experiments with Undiluted Complex. The intensity *I* of the ESR signal of a system of dimers as a function of temperature is given by *Eqn. 2* where *J* is the exchange constant between the two spins in the dimer [16]. A plot of the reciprocal ESR intensity of

$$I \propto \frac{1}{T-\theta}\left\{1+\frac{1}{3}\cdot\exp\frac{-2J}{kT}\right\}^{-1} \tag{2}$$

2 as a function of temperature is reproduced in *Fig. 5*. The linear relationship observed up to a temperature of 6 K excludes the presence of any significant antiferromagnetic exchange between the two Cu-centers of the dimer. The presence of a weak ferromagnetic interaction between the two Cu-atoms is, however, difficult to exclude with certainty from such a plot [16]. There is no precedent for a dimeric Cu^{II} *Schiff*-base structure which involves the imino N-atoms as out-of-plane bridging atoms[3]), and no useful comparison can be made with respect to the observed magnetic properties of this system. Most *Schiff*-base metal dimer complexes show a weak antiferromagnetic exchange interaction

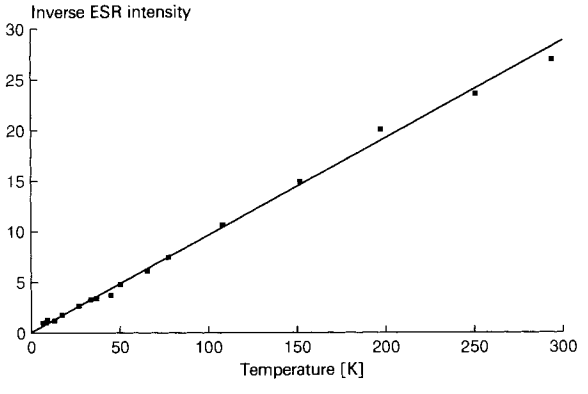

Fig. 5. *Plot of the reciprocal ESR intensity as a function of temperature*

[3]) ESR studies of *N,N'*-phenylenebis(*o*-aminobenzylideneiminato)copper(II) and *N,N'*-ethylenebis(*o*-aminobenzylideneiminato)copper(II) have been reported in $CHCl_3$/toluene solution at 77 K. Dimer formation is believed to occur *via* the imino N-atoms (see [17]).

[7], notable exceptions being [Cu(salen)] and [Cu(Mesal)$_2$] which show ferromagnetic exchange of magnitudes $2J = +18$ and $+8$ cm^{-1}, respectively [18]. The absence of such an exchange in complex **2** could be due to the relatively weak out-of-plane interaction between the N- and Cu-atoms. It has been suggested that out-of-plane bonding between Cu and O at distances greater than 2.8 Å are too long to transmit any significant exchange interaction [19]. It should, however, be noted that exchange coupling between two paramagnetic centers has been observed at considerably longer distances with [20] or without a bridging ligand [21].

Experimental Part

General. [Fe(η^5-C_5H_5)(CO)$_2$(NH_3)][PF_6] was prepared in the same manner as the tetraphenylborate salt [22], but using $NH_4[PF_6]$. Macrocycles *(9,10,12,13,15,16-hexahydro-3,7:18,22-dimetheno-8,11,14,17,1,24-benzotetraoxadiazacyclohexacosine-29,30-diolato(2-)-*N^1,N^{24},O^{29},O^{30}*)copper(II) and -nickel(II)* (**1a** and **1b**, resp.) were synthesized by literature procedures [2]. IR spectra (cm^{-1}): *Perkin-Elmer-298* spectrophotometer. ^{1}H-NMR spectra (δ in ppm): *Bruker-AC-250* spectrometer.

*[{Fe(η^5-C_5H_5)(CO)$_2$(NH_3)} ⊂ **1a**][PF_6]* (**2**). To a soln. of [Fe(η^5-C_5H_5)(CO)$_2$(NH_3)][PF_6] (0.162 g, 0.48 mmol) in THF (80 ml) was added a soln. of **1a** (0.250 g, 0.48 mmol) in $CHCl_3$ (300 ml). The resulting orange-green soln. was purged with N_2 and then allowed to stand in the dark under N_2 for 10 days. Two crystalline morphologies were obtained, dark red rhombic crystals and yellow plates, resulting in a combined yield of 0.282 g (68%). A suitable crystal of rhombic morphology was selected for an X-ray crystal-structure determination. The yellow plate-like crystals analyzed correctly for a 1:1 host-guest complex. IR (nujol mull, NaCl) 2025, 1960 (CO). Anal. calc. for $C_{33}H_{32}CuF_6FeN_3O_8P \cdot 0.5CHCl_3$: C 43.61, H 3.55, Cu 6.89, F 12.35, Fe 6.05, N 4.55, P 3.36; found: C 42.35, H 3.47, Cu 6.78, F 12.46, Fe 5.86, N 4.37, P 3.13.

*[{Fe(η^5-C_5H_5)(CO)$_2$(NH_3)} ⊂ **1b**][PF_6]* (**3**). As described for **2** from [Fe(η^5-C_5H_5)(CO)$_2$(NH_3)][PF_6] (0.162 g, 0.48 mmol) and **1b** (0.250 g, 0.48 mmol). After standing for 3 days, filtration gave 0.280 g (68%) of dark violet crystals. IR (KBr): 2025, 1960 (CO). ^{1}H-NMR ((D$_6$)DMSO): 8.87 (br. *s*, 2H, N=CH); 8.15 (br. *s*, 2H, Ar'H); 7.37–6.57 (*m*, 8H, Ar'H, ArH); 5.37 (*s*, C_5H_5); 4.00 (br. *s*, 4H, ArOCH_2); 3.78–3.77 (*m*, 4H, CH_2O); 3.68 (*s*, 4H, CH_2O); 2.64 (br. *s*, NH_3). Anal. calc. for $C_{33}H_{32}F_6FeN_3NiO_8P \cdot CH_3Cl$: C 41.78, H 3.40, F 11.66, Fe 5.71, N 4.30, Ni 6.01, P 3.17; found: C 41.98, H 3.57, F 11.43, Fe 5.71, N 4.43, Ni 6.05, P 3.03.

X-Ray Crystal-Structure Determination. Crystal data: $[C_7H_8FeNO_2 \cdot C_{26}H_{24}CuN_2O_6][PF_6]$, triclinic, space group *P*I, $a = 9.850(1)$, $b = 9.866(1)$, $c = 18.176(2)$ Å, $\alpha = 103.97(1)$, $\beta = 99.16(1)$, $\gamma = 89.66(1)°$, $V = 169(1)$ Å^3, $Z = 2$, $D_{calc} = 1.694$ g · cm^{-3}. A *Philips-PW-1100* automatic diffractometer was used for data collection at 190 K with Mo$K\alpha$ radiation and graphite monochromator. The intensities of 6195 independent reflections with $\Theta < 25°$ were measured, of which 4168 were classified as observed with $I > 3\sigma(I)$. The structure was solved by direct methods (SDP MULTAN 82) [23]. The structure was resolved by full-matrix least-squares calculation with anisotropic thermal parameters for the non-H-atoms. The H-atoms were calculated at idealized positions and included with fixed parameters in the structure-factor calculation. The 478 parameters converged at an *R* value of 0.0449. Final fractional coordinates and supplementary material were deposited with the *Cambridge Crystallographic Data Centre.*

ESR and ENDOR Measurements. ESR experiments were performed on a *Varian-E9* ESR spectrometer equipped with an *Oxford-Instruments* continuous-flow cryostat *ESR 910* and a temperature controller *ITC4*. The pulsed ENDOR spectrometer [24] and the pulse sequences applied in these experiments have been previously described [13]. In the *Mims*-ENDOR experiment [13], a sequence of 3 microwave pulses was used ($\pi/2$, $\pi/2$, $\pi/2$) with nominal flip angles of $\pi/2$, a length of *ca.* 20 ns, and a delay time between the first two pulses of 350 ns. The radio-frequency pulse (length, 10 μs) was applied between the 2nd and the 3rd microwave pulse. The *Davies*-ENDOR experiment was performed with a sequence of 3 microwave pulses (nominal flip angles: $\pi/2$, $\pi/2$, $\pi/2$) and applying the radio-frequency pulses (10 μs) between the 1st and the 2nd microwave pulse. In both experiments, the intensity of the electron-spin echoes after the 3rd microwave pulse were observed at 10 K as a function of the radio frequency.

We would like to thank *T. Lochmann* and *H. R. Walter* for technical assistance.

REFERENCES

[1] a) H. M. Colquhoun, J. F. Stoddart, D. J. Williams, *Angew. Chem. Int. Ed.* **1983,** *25,* 487; b) H. M. Colquhoun, D. F. Lewis, J. F. Stoddart, D. J. Williams, *J. Chem. Soc., Dalton Trans.* **1983,** 607.

[2] C. J. van Staveren, J. van Eerden, F. C. van Veggel, S. Harkema, D. N. Reinhoudt, *J. Am. Chem. Soc.* **1988,** *110,* 4994.

[3] E. Keller, 'Schakal88. A Program for the Graphic Representation of Molecular and Crystallographic Models', Kristallographisches Institut der Universität Freiburg, D–7800 Freiburg.

[4] K. N. Trueblood, C. B. Knobler, D. S. Lawrence, R. V. Stevens, *J. Am. Chem. Soc.* **1982,** *104,* 1355.

[5] M. Chikira, H. Yokoi, T. Isobe, *Bull. Chem. Soc. Jpn.* **1974,** *47,* 2208.

[6] a) D. Hall, S. V. Sheat, T. N. Waters, *J. Chem. Soc. (A)* **1968,** 460; b) H. Montgomery, B. Morosin, *Acta Crystallogr.* **1961,** *14,* 551; c) E. C. Lingafelter, G. L. Simmons, B. Morosin, C. Scheringer, C. Freiburg, *ibid.* **1961,** *14,* 1222; d) D. Hall, T. N. Waters, *J. Chem. Soc.* **1960,** 2644.

[7] D. J. Hodgson, *Prog. Inorg. Chem.* **1975,** *19,* 173.

[8] E. N. Baker, D. Hall, T. N. Waters, *J. Chem. Soc. (A)* **1970,** 406.

[9] G. R. Clark, D. Hall, T. N. Waters, *J. Chem. Soc. (A)* **1968,** 223.

[10] E. N. Baker, D. Hall, T. N. Waters, *J. Chem. Soc. (A)* **1970,** 400.

[11] G. H. Rist, J. S. Hyde, *J. Chem. Phys.* **1970,** *52,* 4633.

[12] a) S. Kita, M. Hashimoto, M. Iwaizumi, *Inorg. Chem.* **1979,** *18,* 3432; b) M. I. Scullane, H. C. Allen, Jr., *J. Coord. Chem.* **1975,** *4,* 255.

[13] A. Grupp, M. Mehring, 'Modern Pulsed and Continuous-Wave Electron Spin Resonance', Eds. L. Kevan and M. K. Bowman, John Wiley, New York, 1990, p. 195–230.

[14] M. Iwaizumi, T. Kudo, S. Kita, *Inorg. Chem.* **1986,** *25,* 1546.

[15] J. Ammeter, G. Rist, Hs. H. Günthard, *J. Chem. Phys.* **1972,** *57,* 3852.

[16] R. L. Carlin, 'Magnetochemistry', Springer-Verlag, Berlin–Heidelberg, 1986, p. 76–77.

[17] A. D. Toy, M. D. Hobday, P. D. Boyd, T. D. Smith, J. R. Pilbrow, *J. Chem. Soc., Dalton Trans.* **1973,** 1259.

[18] W. E. Hatfield, *Inorg. Chem.* **1972,** *11,* 216.

[19] G. W. Inman, Jr., W. E. Hatfield, R. F. Drake, *Inorg. Chem.* **1972,** *10,* 2425.

[20] W. E. Hatfield, P. Singh, F. Nepveu, *Inorg. Chem.* **1990,** *29,* 4214.

[21] P. J. Barker, S. R. Stobart, *J. Chem. Soc., Chem. Commun.* **1980,** 969.

[22] E. O. Fischer, E. Moser, *Inorg. Synth.* **1970,** *13,* 35.

[23] 'Enraf-Nonius 1987. Structure Determination Package', Delft; P. Main, S. E. Fiske, L. Hull, J. Lessinger, G. Germain, J. P. Declercq, M. M. Woolfson, 'MULTAN 82. A System of Computer Programs for the Automatic Solution of Crystal Structures from X-Ray Diffraction Data', University of York, England, and Louvain, Belgium, 1982.

[24] J. Forrer, S. Pfenninger, J. Eissenegger, A. Schweiger, *Rev. Scient. Instrum.* **1990,** *61,* 3360.